UCLA
UCLA Previously Published Works

Title

18F-FDG PET Visualizes Systemic STING Agonist-Induced Lymphocyte Activation in Preclinical Models

Permalink

https://escholarship.org/uc/item/9w54v9cm

Journal

Journal of Nuclear Medicine, 64(1)

ISSN

0161-5505

Authors

Le, Thuc M

Lee, Hailey R

Abt, Evan R

et al.

Publication Date

2023

DOI

10.2967/jnumed.122.264121

Peer reviewed

^{18}F-FDG PET Visualizes Systemic STING Agonist-Induced Lymphocyte Activation in Preclinical Models

Thuc M. Le*[1,2], Hailey R. Lee*[1,2], Evan R. Abt[1,2], Khalid Rashid[1,2], Amanda L. Creech[1,2], Keke Liang[3], Jing Cui[4], Arthur Cho[5], Liu Wei[1,2], Amanda Labora[6,7], Charlotte Chan[6], Eric Sanchez[1,2], Kriti Kriti[8], Daniel Karin[1,2], Luyi Li[6], Nanping Wu[6], Christine Mona[1,2], Giuseppe Carlucci[1,2], Willy Hugo[7,9], Ting-Ting Wu[1], Timothy R. Donahue[1,2,6,7,10], Johannes Czernin[1,2,7,10], and Caius G. Radu[1,2,7,10]

[1]Molecular and Medical Pharmacology, UCLA, Los Angeles, California; [2]Ahmanson Translational Imaging Division, UCLA, Los Angeles, California; [3]Department of Pancreatic and Thyroidal Surgery, Shengjing Hospital, China Medical University, Shenyang, China; [4]Department of Pancreatic Surgery, Union Hospital, Tongji Medical College, Huazhong University of Science and Technology, Hubei, China; [5]Department of Nuclear Medicine, Yonsei University College of Medicine, Seoul, South Korea; [6]Department of Surgery, UCLA, Los Angeles, California; [7]David Geffen School of Medicine, UCLA, Los Angeles, California; [8]Elucidata Corporation, Cambridge, Massachusetts; [9]Division of Dermatology, Department of Medicine, UCLA, Los Angeles, California; and [10]Jonsson Comprehensive Cancer Center, UCLA, Los Angeles, California

Stimulator of interferon genes (STING) is a mediator of immune recognition of cytosolic DNA, which plays important roles in cancer, cytotoxic therapies, and infections with certain pathogens. Although pharmacologic STING activation stimulates potent antitumor immune responses in animal models, clinically applicable pharmacodynamic biomarkers that inform of the magnitude, duration, and location of immune activation elicited by systemic STING agonists are yet to be described. We investigated whether systemic STING activation induces metabolic alterations in immune cells that can be visualized by PET imaging. **Methods:** C57BL/6 mice were treated with systemic STING agonists and imaged with ^{18}F-FDG PET after 24 h. Splenocytes were harvested 6 h after STING agonist administration and analyzed by single-cell RNA sequencing and flow cytometry. ^{18}F-FDG uptake in total splenocytes and immunomagnetically enriched splenic B and T lymphocytes from STING agonist–treated mice was measured by γ-counting. In mice bearing prostate or pancreas cancer tumors, the effects of STING agonist treatment on ^{18}F-FDG uptake, T-lymphocyte activation marker levels, and tumor growth were evaluated. **Results:** Systemic delivery of structurally distinct STING agonists in mice significantly increased ^{18}F-FDG uptake in the spleen. The average spleen SUV$_{max}$ in control mice was 1.90 (range, 1.56–2.34), compared with 4.55 (range, 3.35–6.20) in STING agonist–treated mice ($P < 0.0001$). Single-cell transcriptional and flow cytometry analyses of immune cells from systemic STING agonist–treated mice revealed enrichment of a glycolytic transcriptional signature in both T and B lymphocytes that correlated with the induction of immune cell activation markers. In tumor-bearing mice, STING agonist administration significantly delayed tumor growth and increased ^{18}F-FDG uptake in secondary lymphoid organs. **Conclusion:** These findings reveal hitherto unknown functional links between STING signaling and immunometabolism and suggest that ^{18}F-FDG PET may provide a widely applicable approach toward measuring the pharmacodynamic effects of systemic STING agonists at a whole-body level and guiding their clinical development.

Key Words: STING agonists; ^{18}F-FDG PET; lymphocytes; immune activation; immunometabolism

Stimulator of interferon genes (STING) is an essential component of an evolutionarily conserved nucleic acid–sensing machinery (*1*). STING functions downstream of cyclic guanosine monophosphate and adenosine monophosphate synthase, a sensor for damaged self-cytosolic or foreign double-stranded DNA associated with cellular stress phenotypes such as infection and malignant transformation (*2,3*). Studies showing the antitumor effects exerted by pharmacologic STING activation (*4*) have provided the impetus for the development of small-molecule STING agonists as a new class of immunooncology agents. Although first-generation STING agonists have advanced to clinical trials for the treatment of cancer, the requirement for intratumoral administration has limited their utility (*4*).

Recently, several groups have developed second-generation STING agonists amenable to systemic (intravenous or oral) administration (*4–6*). In mice, systemic STING activation by these new immunostimulatory agents exerts potent antitumor effects (*5–8*). However, significant questions remain regarding how to optimally dose and schedule systemic STING agonists to maximize their therapeutic efficacy while minimizing the potential risk of toxic effects resulting from overstimulation. Moreover, sustained overactivation of STING is known to induce lymphopenia and T-cell exhaustion (*9,10*) and has been shown to impair the development of durable antitumor immunity (*7*). Therefore, there is a need to develop clinically applicable pharmacodynamic biomarkers to determine the magnitude, duration, and location of immune activation elicited by systemic STING agonists. Identification of metabolic alterations induced by STING activation may guide the development of such pharmacodynamic biomarkers. Accordingly, we showed that STING activation in pancreatic ductal adenocarcinoma cells exerts profound effects on nucleotide metabolism by upregulating genes involved in nucleotide catabolism and that STING-mediated metabolic reprogramming of pancreatic ductal adenocarcinoma tumors can be imaged by ^{18}F-fluorothymidine

PET (*11*). Although this study identified ^{18}F-fluorothymidine as a pharmacodynamic PET biomarker of interferon signaling in pancreatic ductal adenocarcinoma cells, it is conceivable that STING activation in immune cells may induce additional metabolic alterations.

To identify metabolic PET biomarkers of STING activation in immune cells, we considered that STING and toll-like receptors share similar downstream effectors, with both classes of pattern recognition receptor triggering the production of type I interferons and nuclear factor-κB–dependent cytokines (*12–14*). Furthermore, recent studies have shown that systemic toll-like receptor 4, 7, and 9 agonists increase splenic ^{18}F-FDG uptake (*12–14*). Here, we investigated whether ^{18}F-FDG PET imaging is also sensitive to STING activation in immune cells in secondary lymphoid tissues. To identify the immune cell types impacted by systemic STING activation and delineate potential mechanisms responsible for changes in ^{18}F-FDG uptake in these cells, we performed single-cell transcriptomic analyses of splenocytes isolated from STING agonist–treated mice. We investigated whether changes in splenic ^{18}F-FDG uptake induced by STING activation correlate with the expression of T and B lymphocyte activation markers. We also examined whether interferon signaling, which is strongly upregulated in T and B lymphocytes after STING activation, is required for changes in ^{18}F-FDG uptake triggered by systemic STING agonists in these immune cell populations. Finally, we examined whether systemic STING activation increases ^{18}F-FDG uptake in secondary lymphoid tissues in tumor-bearing mice and whether these effects correlate with tumor responses.

Collectively, our findings identify new functional connections between STING activation and immunometabolism and suggest that ^{18}F-FDG PET imaging provides a readily translatable biomarker to assess the magnitude and duration of the effects induced in lymphocytes by systemic STING agonists.

MATERIALS AND METHODS

Animal Studies

All animal studies were approved by the UCLA Animal Research Committee and were performed according to the guidelines of the UCLA Department of Laboratory Animal Medicine. C57BL/6 mice 6–8 wk old were acquired from Jackson Laboratory (stock no. 000664). Type I interferon-α/IFNβ receptor knockout (*Ifnar* KO) mice were donated by Genhong Cheng (UCLA). The animals were treated intravenously with diaminobenzimidazole (diABZI) (catalog no. S8796 [Selleckchem], prepared in 40% PEG400 in saline) or, via oral gavage, with 4-(5,6-dimethoxy-1-benzothiophen-2-yl)-4-oxobutanoic acid (MSA-2) (catalog no. S9681 [Selleckchem], prepared in phosphate-buffered saline, 200 mg/kg).

PET/CT

PET and CT images were acquired in sequence using a G8 PET/CT scanner (PerkinElmer/Sofie Biosciences) 1 h after administration of 0.74 MBq of ^{18}F-FDG. The mice were kept fasting for 4 h before probe administration. PET data were analyzed using the PMOD (version 3.612; PMOD Technologies Ltd.) and Osirix (Pixmeo) software packages. A volume of interest was drawn (spleen and lymph nodes), and SUV_{max} was recorded to quantify ^{18}F-FDG uptake.

γ-Counting

Spleen and lymph nodes (brachial and inguinal) were isolated 1 h after the administration of 9.25 MBq of ^{18}F-FDG. Tissues or single-cell suspensions were placed in scintillation vials for radioactivity measurements by γ-counting (Wizard2; PerkinElmer).

Cell Lines

RM1 cells were purchased from American Type Culture Collection, and the KP4662 $Kras^{G12D/+}$ line was a gift from Robert Vonderheide at the University of Pennsylvania. The KP4662 $Kras^{G12C/-}$ cell is hemizygous for the $Kras^{G12C}$ and was derived from KP4662 $Kras^{G12D/+}$ using CRISPR technology (CRISPR Therapeutics) to replace the $Kras^{G12D}$ allele. All cell lines were cultured in Dulbecco modified Eagle medium with 10% fetal bovine serum and L-glutamine at 37°C and 5% CO_2. For tumor growth experiments, mice were injected subcutaneously with 0.5×10^6 RM1 cells for RM1 or with 1×10^6 KP4662 cells. Tumor volumes were calculated by (width^2 × length)/2 using masked caliper measurements. Excised tumors were dissociated using the Miltenyi GentleMACS dissociator.

Enzyme-Linked Immunosorbent Assay

Serum interferon β (IFNβ) levels were measured by enzyme-linked immunosorbent assay (catalog no. 42400; PBL Assay Science) per manufacturer instructions.

Flow Cytometry

A detailed description of the protocol and reagents is provided in the supplemental materials.

CD4$^+$, CD8$^+$ T-Cell, and B-Cell Enrichments

Target cells were enriched using magnetic separation (OctoMACS separator [Miltenyi], catalog no. 130042108) per manufacturer instructions. The beads used were CD4 (L3T4) mouse microbeads (catalog no. 130117043), CD8 (Ly-2) mouse microbeads (catalog no. 130117044), and CD43 (Ly-48) mouse microbeads (catalog no. 130-049-801).

Single-Cell RNA Sequencing (scRNA-Seq) Analysis

A detailed description of the analysis pipeline is provided in the supplemental materials (*15,16*).

Statistical Analysis

Data are presented as mean ± SD, with the number of biologic replicates indicated. Comparisons of 2 groups were evaluated using the unpaired 2-tailed Student *t* test, and *P* values of less than 0.05 were considered significant. Comparisons of more than 2 groups were assessed using 1-way ANOVA followed by Bonferroni adjustment, and *P* values of less than 0.05/m, where m is the total number of possible comparisons, were considered significant.

RESULTS

Systemic STING Agonists Increase Splenic ^{18}F-FDG Uptake

Systemic administration of a STING agonist (diABZI compound 3 (*5*), 1.5 mg/g intravenously) significantly increased splenic ^{18}F-FDG uptake as measured in vivo by PET (Fig. 1A). Similar increases in splenic ^{18}F-FDG uptake were induced by MSA-2, a systemic STING agonist (*6*) structurally distinct from diABZI (Fig. 1B). We then compared the persistence of increased ^{18}F-FDG uptake in the spleen with the induction of IFNβ in serum, a commonly used indicator of pharmacologic STING activation (*5,6*). Serum IFNβ levels increased 6 h after systemic STING agonist treatment and dropped rapidly by approximately 3 orders of magnitude, approaching baseline levels at the 24-h time point (Fig. 1C). In contrast, splenic ^{18}F-FDG uptake peaked 24 h after STING agonist treatment and persisted for at least 48 h (Fig. 1D). Collectively, these data indicate that ^{18}F-FDG accumulation in the spleen as measured by PET is a potential noninvasive biomarker for systemic STING agonists that provides information about the location and duration of STING activation in immune cells that cannot be obtained by monitoring serum interferon levels alone.
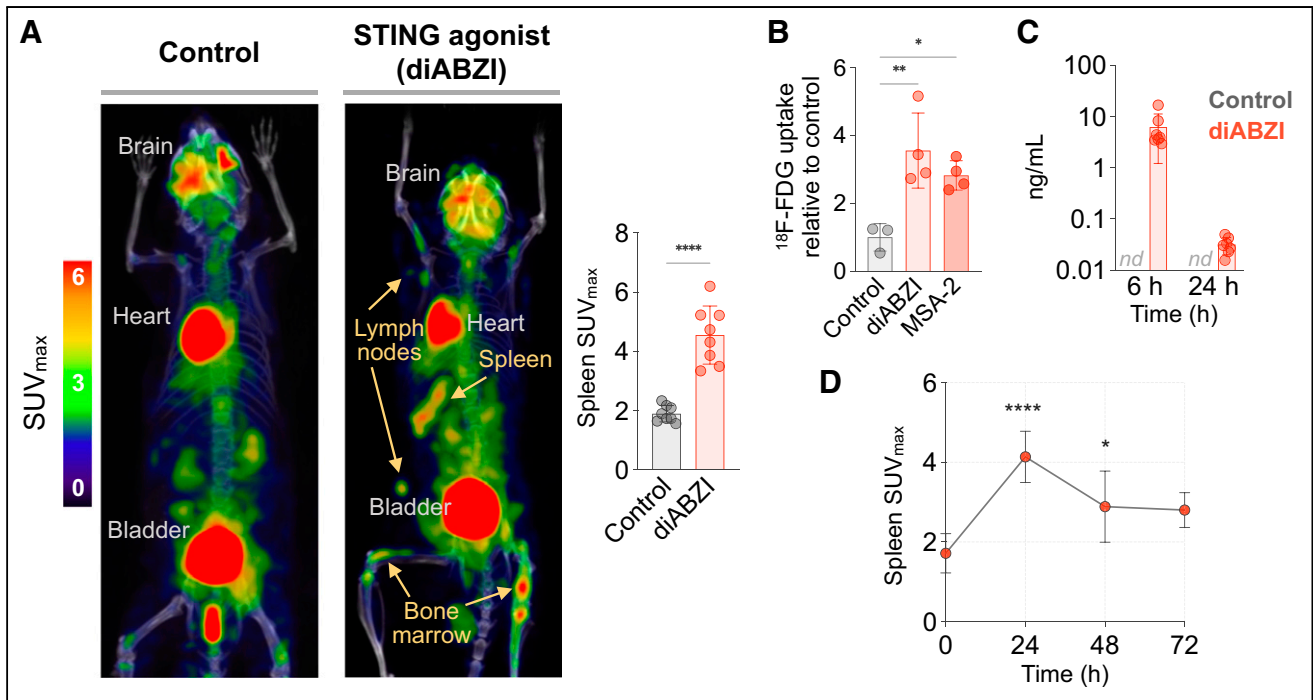
FIGURE 1. Systemic STING agonist treatment increases ^{18}F-FDG uptake in spleen. (A) Representative ^{18}F-FDG PET scans of control and STING agonist–treated (diABZI, 1.5 mg/kg intravenously) C57BL/6 mice at 24 h with quantification (8 mice per group). (B) Ex vivo γ-counter quantification of ^{18}F-FDG uptake in spleens isolated from mice treated with vehicle control, diABZI (1.5 mg/kg intravenously), or MSA-2 (200 mg/kg orally) (3–4 mice per group). (C) IFNβ production in response to diABZI treatment (1.5 mg/kg intravenously). Serum collected at indicated time points was assayed by enzyme-linked immunosorbent assay for IFNβ levels (7 mice per group). (D) Quantification of splenic ^{18}F-FDG uptake of STING agonist–treated mice (diABZI, 1.5 mg/kg intravenously) at 0–72 h (5 mice). n.d. = not detected. $^*P < 0.05$. $^{**}P < 0.01$. $^{****}P < 0.0001$.

Systemic STING Activation Induces Glycolysis-Related Gene Expression in T and B Cells

To further investigate the impact of systemic STING activation on splenic immune populations and identify the cell types responsible for the increased ^{18}F-FDG accumulation, we examined transcriptional changes induced by STING agonists using scRNA-seq. An integrated uniform manifold approximation and projection plot of splenocytes isolated from mice treated with a systemic STING agonist (diABZI) or with a vehicle control revealed a shift in the localization of T and B lymphocyte clusters in the diABZI group compared with the control group, indicative of substantial STING agonist–induced transcriptional alterations in these immune cell populations (Fig. 2A; Supplemental Figs. 1A–B). We then assessed splenic T- and B-lymphocyte populations for gene expression changes linked to ^{18}F-FDG accumulation. We observed significant upregulation of hexokinase 1 (*Hk1*) in T lymphocytes and *Hk2* in B lymphocytes (Fig. 2B). Expression of other glycolytic genes was affected to varying degrees by systemic STING activation (Supplemental Fig. 1C). Consistent with the upregulation of *Hk* isoforms in T and B lymphocytes, systemic STING agonist treatment also increased the expression of *Hif1a* and *Myc*, 2 major transcriptional regulators of *Hk1* and *Hk2* (*17–20*). To confirm that T and B lymphocytes are indeed responsible for the increased ^{18}F-FDG accumulation induced by systemic STING activation, we treated mice with diABZI and 24 h later injected them with ^{18}F-FDG (9.25 MBq). After 1 h, we immunomagnetically enriched splenic CD4$^+$ and CD8$^+$ T lymphocytes and B lymphocytes and measured ^{18}F-FDG uptake by γ-counting. Consistent with the scRNA-seq analysis, significant increases in

^{18}F-FDG accumulation were observed in all 3 immune populations isolated from systemic STING agonist–treated mice (Supplemental Fig. 2). These findings indicate that T and B lymphocytes, which account for most immune cells in the spleen, are responsible for increased splenic ^{18}F-FDG uptake after systemic STING agonist treatment.

Activation Markers in Lymphocytes Correlate with Splenic ^{18}F-FDG Uptake After Systemic STING Activation

Next, we determined whether systemic STING agonist–induced changes in ^{18}F-FDG accumulation by splenic T and B lymphocytes correlate with immune activation markers. First, we probed for transcriptional upregulation of selected activation markers in our scRNA-seq dataset and found that *Cxcl10* and *Cd69* were induced by STING activation in both T and B lymphocytes (Fig. 3). B lymphocytes increased the expression of the costimulatory molecule *Cd86*. T and B lymphocytes from STING agonist–treated mice also showed significant induction of *Cd274*, the gene encoding for the programmed-death ligand 1 (PD-L1), and *Lag3*, which are both associated with immune inhibitory and exhaustion phenotypes (Fig. 3) (*21,22*).

Next, we used flow cytometry to determine whether transcriptional alterations in the expression of immune activation and inhibitory/exhaustion markers induced by systemic STING agonist treatment correlate with changes in splenic ^{18}F-FDG uptake. For this, we determined cell surface CD69 and PD-L1 expression alongside ^{18}F-FDG uptake in splenocytes from mice treated with various doses of diABZI (Supplemental Fig. 3). Both the splenic ^{18}F-FDG uptake and the level of immune markers, CD69 and PD-L1, increased in a dose-dependent manner in splenic CD4$^+$, CD8$^+$ T, and B cells, leading to a
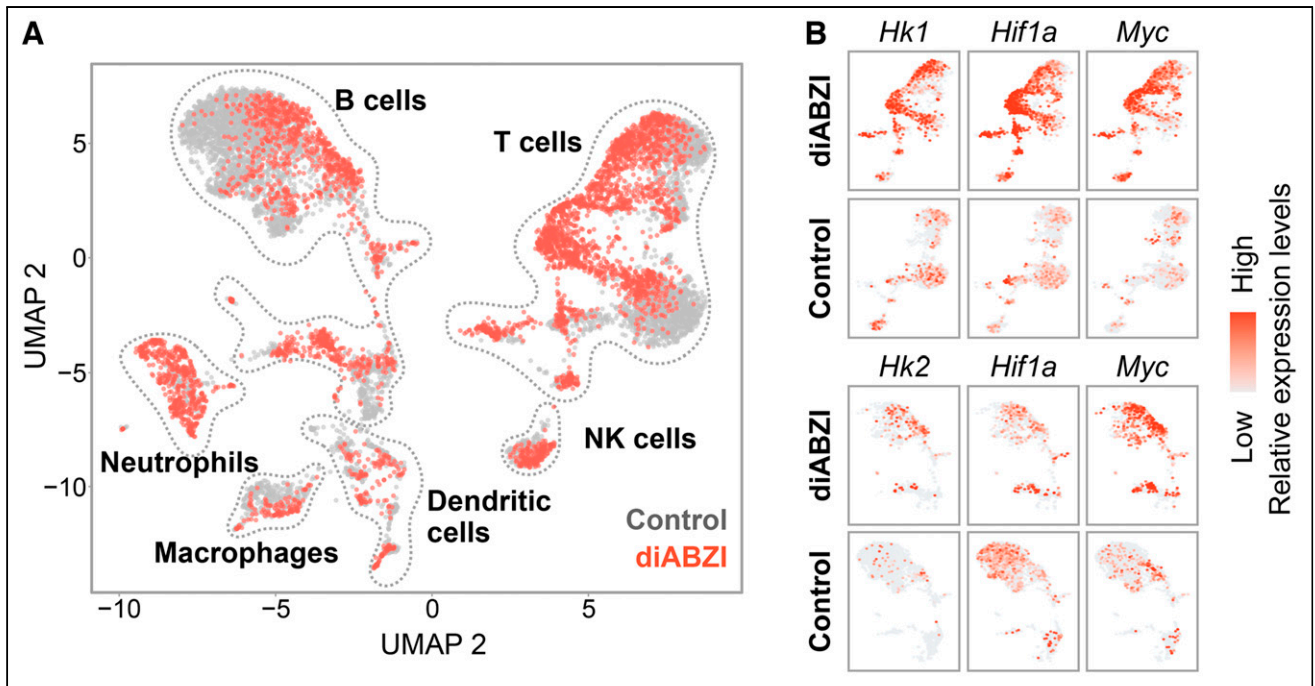
FIGURE 2. Identification of cell populations responsible for increased splenic ^{18}F-FDG uptake after systemic STING activation. (A) Uniform manifold approximation and projection of transcriptional profiles of control (6,701 splenocytes) and STING agonist–treated mice (4,381 splenocytes). Major cell subsets are indicated; Supplemental Figure 2 and the supplemental methods provide details. (B) Transcriptional induction of genes related to glycolytic metabolism in T-cell and B-cell subsets. NK = natural killer; UMAP = uniform manifold approximation and projection.

strong correlation (Fig. 4). A similar pattern was observed in lymph nodes (Supplemental Fig. 4). Collectively, these data indicate that systemic STING agonist–induced ^{18}F-FDG accumulation in secondary lymphoid organs measured by PET provides a reliable metabolic correlate of phenotypic changes associated with activated immune markers in major lymphocyte populations.

Splenic ^{18}F-FDG Uptake Induced by Systemic STING Activation Does Not Require Interferon Signaling

Ontologic analysis of the top 100 positively enriched genes across splenic immune cell clusters by scRNA-seq revealed a dominant role for interferon response in remodeling the transcriptional landscape of immune cells by systemic STING activation
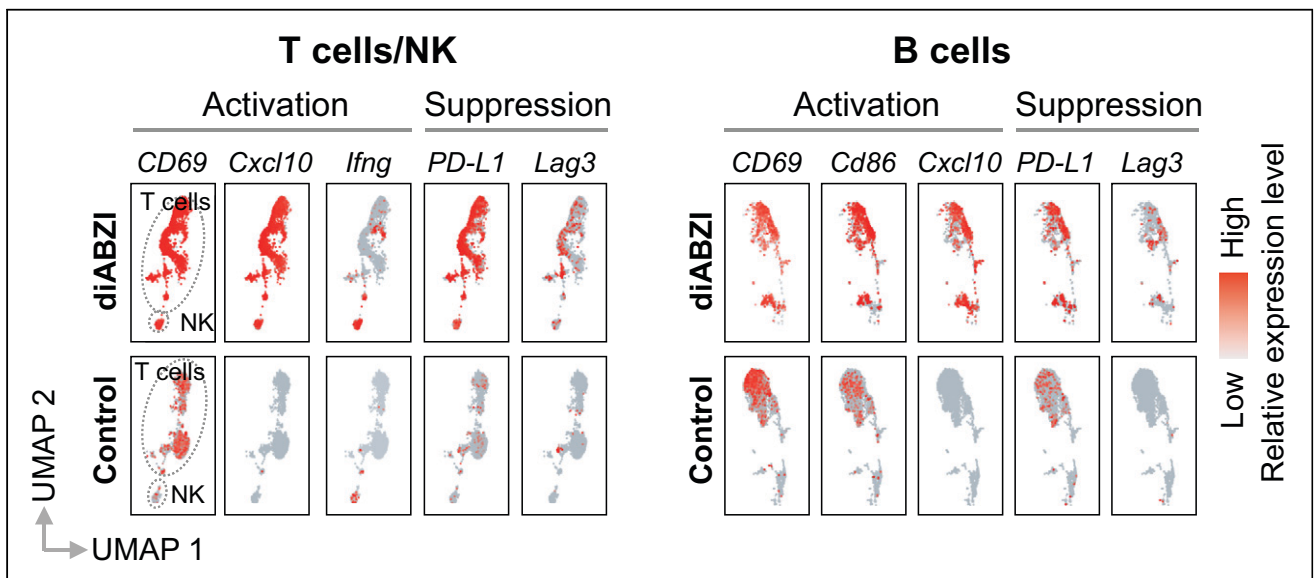

FIGURE 3. Systemic STING activation induces upregulation of immune activation and checkpoint markers in T and B lymphocytes. Induction of immune activation and immune checkpoint/exhaustion gene transcription in T-cell/natural killer–cell subsets and B-cell subsets occurs as indicated by scRNA-seq analysis from Figure 2. NK = natural killer; UMAP = uniform manifold approximation and projection.
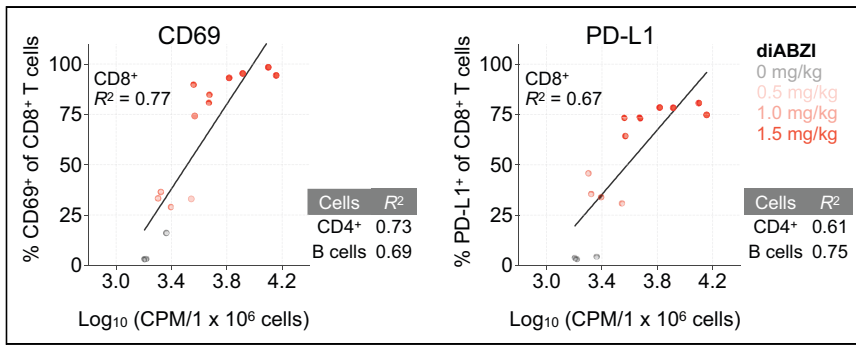
FIGURE 4. Changes in splenic ^{18}F-FDG uptake after systemic STING activation correlate with upregulation of T- and B-cell activation markers. Scatterplots show correlation of log-transformed ex vivo ^{18}F-FDG uptake (x-axis) and CD69 or PD-L1 expression on CD8$^+$ T cells (y-axis). Spearman correlations are summarized in graph.

(Fig. 5A). Given that type I interferons are important downstream effectors of STING activation in immune cells (1), we next investigated whether increased splenic ^{18}F-FDG uptake after STING activation was dependent on interferon signaling using *Ifnar* KO mice. Surprisingly, abolishing interferon signaling in *Ifnar* KO mice did not significantly impact the STING activation–induced increase in splenic ^{18}F-FDG uptake (Fig. 5B). Ex vivo γ-counter measurements of ^{18}F-FDG accumulation in enriched CD4$^+$ and CD8$^+$ T lymphocytes and B cells isolated from the spleens of systemic STING agonist–treated *Ifnar* KO mice were consistent with the in vivo ^{18}F-FDG PET data (Supplemental Figs. 5A–B). Induction of CD69 and PD-L1 was still observed in splenic CD4$^+$, CD8$^+$ T, and B cells from *Ifnar* KO mice treated with STING, suggesting that STING agonist–induced T-cell activation involves pathways other than interferon (Supplemental Fig. 5C). These findings show that STING functions independently of type I interferon signaling to reprogram glucose metabolism and induce activation markers in lymphocytes.
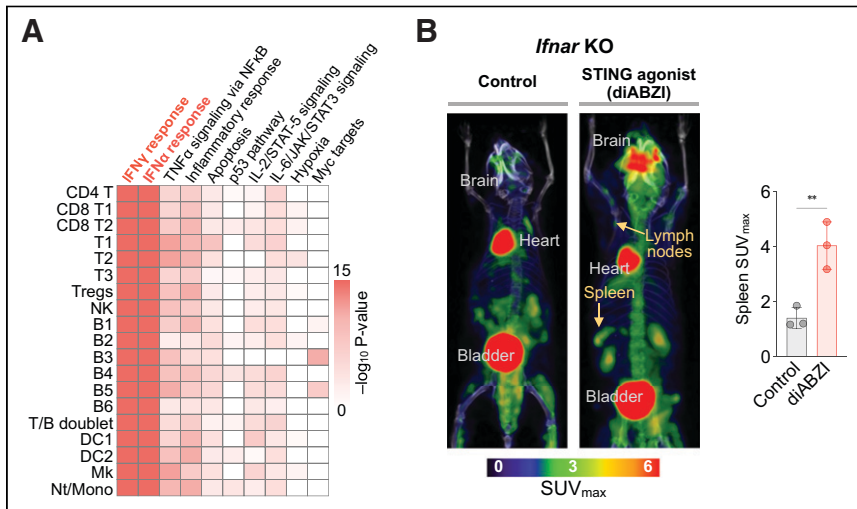
Systemic STING Activation Enhances Splenic ^{18}F-FDG Uptake and T-Cell Activation in Tumor-Bearing Mice

Because systemic STING agonists are currently under clinical investigation for the treatment of cancer (NCT03843359, NCT04096638, NCT03956680), we investigated whether alterations in ^{18}F-FDG uptake and T-lymphocyte activation are detectable in STING agonist–treated tumor-bearing mice and whether these effects correlate with therapeutic responses. STING agonist administration restricted tumor growth in 3 syngeneic tumor models: prostate cancer RM1 and pancreatic cancer KP4662 *Kras*$^{G12D/+}$ and KP4662 *Kras*$^{G12C/+}$ (Fig. 6). Consistent with our findings in tumor-naïve mice, we observed increased ^{18}F-FDG uptake in lymphoid tissues in tumor-bearing mice, including the spleen and lymph nodes (Figs. 7A–7B). Although tumor ^{18}F-FDG uptake was unchanged in STING agonist–treated mice (Fig. 7B), tumor-infiltrating CD4$^+$ and CD8$^+$ T cells increased CD69 expression 24 h after STING agonist administration to levels that were similar to those detected in T cells from secondary lymphoid organs (Fig. 7C). These findings demonstrate that the effects of systemic STING agonists in promoting immune activation and increased ^{18}F-FDG uptake in secondary lymphoid organs can also be detected in tumor-bearing mice and correlate with therapeutic response.

DISCUSSION

Here, we explored ^{18}F-FDG PET imaging as a novel means of visualizing the effects of systemically delivered STING agonists in mice at a whole-body level. We observed robust and reproducible increases in ^{18}F-FDG uptake in the spleen and lymph nodes of mice 24 h after systemic STING agonist treatment (Fig. 1); these changes were induced by structurally distinct STING agonists and persisted for up to 72 h, significantly longer than observed increases in serum cytokine levels, which thus far have typically been used to monitor the effects of STING activation (Fig. 1) (4–6). To gain mechanistic insight into the immediate perturbations that occur in secondary lymphoid organs after STING agonist administration and identify the immune cell types responsible for increased ^{18}F-FDG uptake in the spleen, we used scRNA-seq T and B lymphocytes from STING agonist–treated mice. An upregulated glycolytic signature was shown, indicating that increased splenic ^{18}F-FDG uptake is attributable primarily to acute lymphocyte activation (Fig. 2; Supplemental Figs. 1 and 2). T and B cells upregulated markers associated with both immune activation and specific immune inhibitory mechanisms after systemic STING activation (Fig. 3). By titrating the dose of the systemic STING agonist, we showed that ^{18}F-FDG uptake

FIGURE 5. Increased splenic ^{18}F-FDG uptake induced by systemic STING activation does not require interferon signaling. (A) Pathway enrichment analysis of differentially expressed genes in splenic cell subsets from scRNA-seq analysis in Figure 2. (B) Representative ^{18}F-FDG PET scans of control and STING agonist–treated *Ifnar* KO mice (3 mice per group). NK = natural killer; T1-3 = distinct T cell subsets; Tregs = regulatory T cells; B1-6 = distinct B cell subsets; T/B doublet = T and B cell doublets; DC1-2 = various dendritic cell subsets; Mk = macrophages; Nt/Mono = neutrophile/monocytes. **$P < 0.01$.
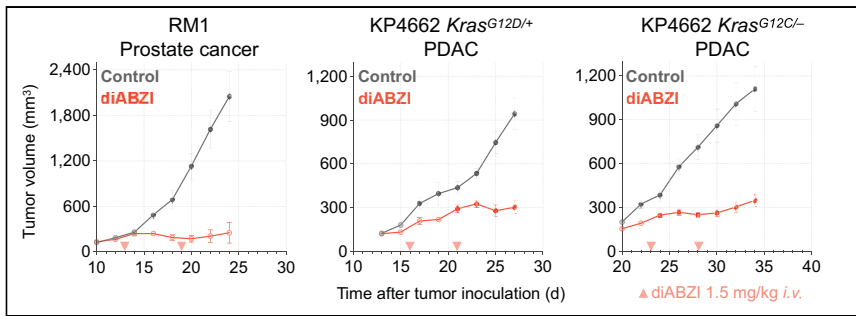
FIGURE 6. Systemic STING activation controls tumor growth. Tumor growth curves from 3 cohorts of C57BL/6J mice bearing subcutaneous RM1, KP4662 Kras[G12D/+], or KP4662 Kras[G12C/+] tumors. Mice were treated with 2 doses of diABZI (1.5 mg/kg intravenously each) as indicated (8 mice per group). PDAC = pancreatic ductal adenocarcinoma.

and immune activation markers increased together in a dose-dependent manner (Fig. 4; Supplemental Figs. 3 and 4). Additionally, we sho wed that reprogramming of lymphocyte glucose metabolism by STING activation occurred independently of interferon signaling (Fig. 5; Supplemental Fig. 5). Finally, we demonstrated that the antitumor efficacy of systemic STING agonists (Fig. 6) was associated with increased ^{18}F-FDG uptake in lymphoid tissues and upregulation of activation markers in T-cell populations, including those infiltrating the tumor (Fig. 7). We suggest that ^{18}F-FDG PET might provide a clinically applicable pharmacodynamic biomarker to guide the dosing and scheduling of systemic STING agonists.

The findings of this study add to a growing body of literature on profound STING effects on cellular metabolism (11,23,24). Previously, we showed that STING activation impacts nucleotide metabolism in pancreatic cancer cells by increasing the expression of thymidine phosphorylase in an interferon-dependent manner (11). Systemic STING activation–induced thymidine phosphorylase

upregulation in human pancreatic cancer xenografts reduced thymidine levels in the tumor microenvironment, which in turn resulted in significantly increased tumor ^{18}F-fluorothymidine uptake (11). Thus, we emphasize that ^{18}F-FDG and ^{18}F-fluorothymidine may provide complementary information regarding the effects of STING agonists. Accordingly, ^{18}F-FDG PET may be the method of choice to measure interferon-independent consequences of STING activation in immune cells. In contrast, ^{18}F-fluorothymidine PET may be the method of choice to determine interferon signaling–dependent effects of systemic STING agonists in tumor cells.

From a mechanistic point of view, our data (Fig. 5; Supplemental Fig. 5) indicate the existence of an interferon signaling–independent link between STING and transcription factors known to regulate glycolysis. In this context, *Myc* and *Hif1a* are transcriptionally induced in T and B cells after STING activation (Fig. 2B). The transcription factor Myc, which regulates the essential glycolytic genes *Glut1, Hk1,* and *Hk2,* is a crucial driver of the glycolytic switch in T-cell activation, as deletion of Myc is sufficient to abolish activation-induced T-cell growth (18). Additionally, hypoxia-inducible factor binds to and stimulates the same set of glycolytic genes (17,19,20,25). Additional studies will be required to elucidate the precise mechanisms by which STING activation leads to interferon signaling–independent increases in HK1 and HK2 expression in T cells and B cells. Nevertheless, ^{18}F-FDG PET/CT may provide a widely available method to noninvasively quantify immune activation induced by systemic STING agonists in both preclinical and clinical settings.
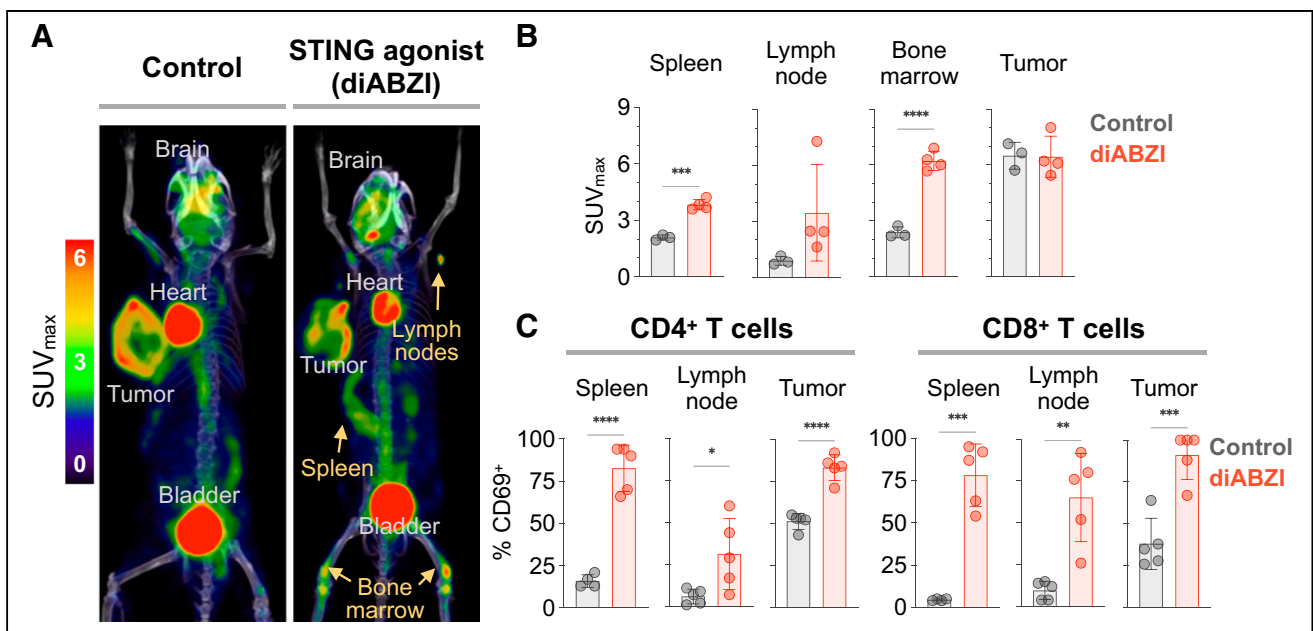

FIGURE 7. Systemic STING activation enhances splenic ^{18}F-FDG uptake in tumor-bearing mice. (A) Representative ^{18}F-FDG PET scans from C57BL/6J mice bearing subcutaneous KP4662 Kras[G12C/−] tumors at 24 d after tumor inoculation. Mice received 0.74-MBq ^{18}F-FDG dose 24 h after STING agonist treatment (diABZI, 1.5 mg/kg intravenously), 1 h before PET scans. (B) Quantification of PET scans from A (3–4 mice per group). (C) Percentage CD69 expression in CD4^{+} and CD8^{+} T cells isolated from spleen, lymph nodes, and KP4662 Kras[G12C/−] tumors. Mice were killed 24 h after treatment (diABZI, 1.5 mg/kg intravenously) for flow cytometry analysis (5 mice per group). $^*P < 0.05$. $^{**}P < 0.01$. $^{***}P < 0.001$. $^{****}P < 0.0001$.

CONCLUSION

These findings reveal hitherto unknown functional links between STING signaling and immunometabolism and suggest that ^{18}F-FDG PET may provide a widely applicable approach toward measuring the pharmacodynamic effects of systemic STING agonists at a whole-body level and guiding their clinical development.

KEY POINTS

QUESTION: Can ^{18}F-FDG PET provide a pharmacodynamic biomarker of immune metabolic reprogramming induced by systemic STING agonists?

PERTINENT FINDINGS: Treatment with structurally distinct systemic STING agonists significantly increased splenic ^{18}F-FDG uptake in mice. Single-cell transcriptional and flow cytometric analyses of immune cells from systemic STING agonist–treated mice revealed an enhanced glycolytic transcriptional signature in T and B lymphocytes, which correlated with the induction of immune activation markers.

IMPLICATIONS FOR PATIENT CARE: ^{18}F-FDG PET imaging may provide a clinically applicable approach to determine the magnitude, duration, and location of immune activation induced by systemic STING agonists currently under development for the treatment of cancer.

REFERENCES

1. Barber GN. STING-dependent cytosolic DNA sensing pathways. *Trends Immunol.* 2014;35:88–93.

2. Barber GN. STING: infection, inflammation and cancer. *Nat Rev Immunol.* 2015; 15:760–770.

3. Li T, Chen ZJ. The cGAS-cGAMP-STING pathway connects DNA damage to inflammation, senescence, and cancer. *J Exp Med.* 2018;215:1287–1299.

4. Chen NN, Zhang H, You QD, Xu XL. Agonist of stimulator of interferon genes as antitumor agents: a patent review (2008-2020). *Expert Opin Ther Pat.* 2021;31: 563–584.

5. Ramanjulu JM, Pesiridis GS, Yang J, et al. Design of amidobenzimidazole STING receptor agonists with systemic activity. *Nature.* 2018;564:439–443.

6. Pan BS, Perera SA, Piesvaux JA, et al. An orally available non-nucleotide STING agonist with antitumor activity. *Science.* 2020;369:eaba6098.

7. Sivick KE, Desbien AL, Glickman LH, et al. Magnitude of therapeutic STING activation determines CD8+ T cell-mediated anti-tumor immunity. *Cell Rep.* 2018; 25:3074–3085.e5.

8. Woo SR, Corrales L, Gajewski TF. The STING pathway and the T cell-inflamed tumor microenvironment. *Trends Immunol.* 2015;36:250–256.

9. Chia J, Eroglu FK, Özen S, et al. Failure to thrive, interstitial lung disease, and progressive digital necrosis with onset in infancy. *J Am Acad Dermatol.* 2016;74: 186–189.

10. Bouis D, Kirstetter P, Arbogast F, et al. Severe combined immunodeficiency in stimulator of interferon genes (STING) V154M/wild-type mice. *J Allergy Clin Immunol.* 2019;143:712–725.e5.

11. Liang K, Abt ER, Le TM, et al. STING-driven interferon signaling triggers metabolic alterations in pancreas cancer cells visualized by [18F]FLT PET imaging. *Proc Natl Acad Sci USA.* 2021;118:e2105390118.

12. Pektor S, Bausbacher N, Otto G, et al. Toll like receptor mediated immune stimulation can be visualized in vivo by [18F]FDG-PET. *Nucl Med Biol.* 2016;43: 651–660.

13. Pektor S, Hilscher L, Walzer KC, et al. In vivo imaging of the immune response upon systemic RNA cancer vaccination by FDG-PET. *EJNMMI Res.* 2018;8:80.

14. Sahin U, Oehm P, Derhovanessian E, et al. An RNA vaccine drives immunity in checkpoint-inhibitor-treated melanoma. *Nature.* 2020;585:107–112.

15. Hao Y, Hao S, Andersen-Nissen E, et al. Integrated analysis of multimodal single-cell data. *Cell.* 2021;184:3573–3587.e29.

16. Durinck S, Spellman PT, Birney E, Huber W. Mapping identifiers for the integration of genomic datasets with the R/Bioconductor package biomaRt. *Nat Protoc.* 2009;4:1184–1191.

17. Nakamura H, Makino Y, Okamoto K, et al. TCR engagement increases hypoxia-inducible factor-1 alpha protein synthesis via rapamycin-sensitive pathway under hypoxic conditions in human peripheral T cells. *J Immunol.* 2005;174:7592–7599.

18. Wang R, Dillon CP, Shi LZ, et al. The transcription factor Myc controls metabolic reprogramming upon T lymphocyte activation. *Immunity.* 2011;35:871–882.

19. Shi LZ, Wang R, Huang G, et al. HIF1alpha-dependent glycolytic pathway orchestrates a metabolic checkpoint for the differentiation of TH17 and Treg cells. *J Exp Med.* 2011;208:1367–1376.

20. Finlay DK, Rosenzweig E, Sinclair LV, et al. PDK1 regulation of mTOR and hypoxia-inducible factor 1 integrate metabolism and migration of CD8+ T cells. *J Exp Med.* 2012;209:2441–2453.

21. Khan AR, Hams E, Floudas A, Sparwasser T, Weaver CT, Fallon PG. PD-L1hi B cells are critical regulators of humoral immunity. *Nat Commun.* 2015;6:5997.

22. Diskin B, Adam S, Cassini MF, et al. PD-L1 engagement on T cells promotes self-tolerance and suppression of neighboring macrophages and effector T cells in cancer. *Nat Immunol.* 2020;21:442–454.

23. Abt ER, Le TM, Dann AM, et al. Reprogramming of nucleotide metabolism by interferon confers dependence on the replication stress response pathway in pancreatic cancer cells. *Cell Rep.* 2022;38:110236.

24. Moore AM, Zhou L, Cui J, et al. NAD+ depletion by type I interferon signaling sensitizes pancreatic cancer cells to NAMPT inhibition. *Proc Natl Acad Sci USA.* 2021;118:e2012469118.

25. Gordan JD, Thompson CB, Simon MC. HIF and c-Myc: sibling rivals for control of cancer cell metabolism and proliferation. *Cancer Cell.* 2007;12:108–113.